Inorganic Chemistry

Article

pubs.acs.org/IC

Changes in the Geometries of C_2H_2 and C_2H_4 on Coordination to CuCl Revealed by Broadband Rotational Spectroscopy and ab-Initio Calculations

Susanna L. Stephens,[†] Dror M. Bittner,[†] Victor A. Mikhailov,[‡] Wataru Mizukami,[‡] David P. Tew,[‡] Nicholas R. Walker,*[,†] and Anthony C. Legon*[,‡]

[†]School of Chemistry, Bedson Building, Newcastle University, Newcastle upon Tyne, Tyne and Wear NE1 7RU, United Kingdom

[‡]School of Chemistry, University of Bristol, Bristol BS8 1TS, United Kingdom

Supporting Information

ABSTRACT: The molecular geometries of isolated complexes in which a single molecule of C_2H_4 or C_2H_2 is bound to CuCl have been determined through pure rotational spectroscopy and ab-initio calculations. The C_2H_2···CuCl and C_2H_4···CuCl complexes are generated through laser vaporization of a copper rod in the presence of a gas sample undergoing supersonic expansion and containing C_2H_2 (or C_2H_4), CCl_4, and Ar. Results are presented for five isotopologues of C_2H_2···CuCl and six isotopologues of C_2H_4···CuCl. Both of these complexes adopt C_{2v}, T-shaped geometries in which the hydrocarbon binds to the copper atom through its π electrons such that the metal is equidistant from all H atoms. The linear and planar geometries of free C_2H_2 and C_2H_4, respectively, are observed to distort significantly on attachment to the CuCl unit, and the various changes are quantified. The $\angle$(*−C−H) parameter in C_2H_2 (where * indicates the midpoint of the C≡C bond) is measured to be 192.4(7)° in the r_0 geometry of the complex representing a significant change from the linear geometry of the free molecule. This distortion of the linear geometry of C_2H_2 involves the hydrogen atoms moving away from the copper atom within the complex. Ab-initio calculations at the CCSD(T)(F12*)/AVTZ level predict a dihedral $\angle$(HCCCu) angle of 96.05° in C_2H_4···CuCl, and the experimental results are consistent with such a distortion from planarity. The bonds connecting the carbon atoms within each of C_2H_2 and C_2H_4, respectively, extend by 0.027 and 0.029 Å relative to the bond lengths in the isolated molecules. Force constants, k_σ, and nuclear quadrupole coupling constants, χ_{aa}(Cu), $[\chi_{bb}(\mathrm{Cu}) - \chi_{cc}(\mathrm{Cu})]$, χ_{aa}(Cl), and $[\chi_{bb}(\mathrm{Cl}) - \chi_{cc}(\mathrm{Cl})]$, are independently determined for all isotopologues of C_2H_2···CuCl studied and for four isotopologues of C_2H_4···CuCl.

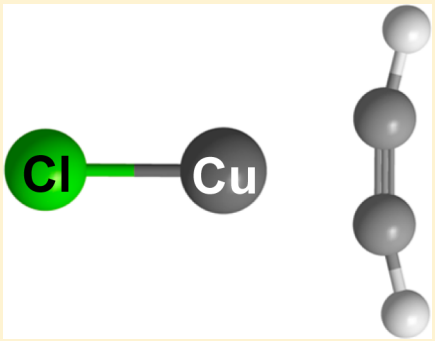

INTRODUCTION

Metal atoms coordinate with alkenes or alkynes through interactions between π electrons of the hydrocarbon and π^* orbitals on the metal.[1,2] The geometries adopted by many coordination complexes depend on the strength and nature of such interactions which can also drive the first step in polymerization or hydrogenation processes.[3] Insight into geometrical changes on formation of complexes can be gained through spectroscopic experiments on model complexes isolated in the gas phase. Bond lengths and angles can be measured with high precision even where units may be difficult or impossible to isolate in the condensed or solution phases. The simple model complexes examined during this work, C_2H_2···CuCl and C_2H_4···CuCl, are generated in the gas phase through laser vaporization of a metal target in the presence of CCl_4 and C_2H_2 or C_2H_4 and stabilized by rapid cooling to a rotational temperature of ∼2 K in the environment of a supersonic gas expansion. This method allows complexes to be generated with a high degree of selectivity and subsequently interrogated while being isolated from the perturbing effects of a solvent or matrix.

Complexes of $M^+(C_2H_2)$ and $M^+(C_2H_4)$ (where M is a metal atom) have previously been generated by laser vaporization and studied by electronic photodissociation spectroscopy. Duncan and co-workers reported C_{2v} geometries for both $Ca^+(C_2H_2)$ and $Mg^+(C_2H_2)$.[4] Kleiber and co-workers reported geometries of the same symmetry for $M^+(C_2H_4)$, where M = Mg, Ca, Zn, and Al.[5] In many cases, the experiments allowed dissociation energies to be determined. Infrared photodissociation spectroscopy was later used to measure vibrational frequencies for $Ni^+(C_2H_2)$, $Co^+(C_2H_2)$, $Fe^+(C_2H_2)$, and $V^+(C_2H_2)$.[6] Photodissociation experiments require measurement of the yield of an ionic photofragment as a function of excitation laser wavelength and are therefore suitable only for ionic complexes. It is also required that energy deposited into complexes by photons efficiently transfers into the dissociative reaction coordinate. Microwave spectroscopy, employed by the present work, does not have the same limitations and carries the advantage that information about individual bond lengths and

Received: August 6, 2014
Published: September 18, 2014

dx.doi.org/10.1021/ic501899c | Inorg. Chem. 2014, 53, 10722−10730

angles can be obtained for neutral molecules with a very high level of precision. It should be noted that microwave spectroscopy can be most readily applied to study molecules with closed-shell electronic states. Coupling interactions in molecules with unpaired electrons yield spectra that can be very challenging to interpret.

The present work follows recent experiments that have quantified changes in the geometries of C_2H_4 and C_2H_2 on coordination of these molecules to the silver atom of an isolated silver halide unit. These studies form part of a wider program to investigate the geometries of complexes where a single Lewis base molecule is coordinated to the metal atom within MX (where M is Cu, Ag, or Au and X is a halogen atom).[7] It was shown that C_2H_4···AgCl adopts a C_{2v} geometry in which C_2H_4 coordinates to the metal atom through its π electrons. The length of the C═C bond within the complex extends relative to that within the C_2H_4 monomer by 0.013 Å (in the r_0 geometry).[7g] The geometry of C_2H_2 is observed to change on coordination to the silver atom of AgCl[7k] and AgCCH,[8] respectively. The C≡C bond is observed to extend by 0.017 Å (in the r_0 geometry) on attachment to AgCl. Hydrogen atoms move away from the silver atom such that the C_2H_2 unit is not linear within the complex and the H−C≡C angle is 187.7(4)°. Similar changes in the structure of C_2H_2 are observed on its attachment to AgCCH where the extension in the C≡C bond length is 0.014 Å (in the r_0 geometry). H atoms move away from the silver atom such that the H−C≡C angle in C_2H_2···AgCCH is 186.0(5)°. The purpose of the present work is the measurement and analysis of the microwave spectra of C_2H_4···CuCl and C_2H_2···CuCl. It will be shown that each complex adopts a C_{2v} geometry in which there is strong interaction between the metal atom and π electrons on the hydrocarbon. Changes in the geometries of C_2H_4 and C_2H_2 on formation of each complex are quantified.

EXPERIMENTAL SECTION

Measurements on each of C_2H_4···CuCl and C_2H_2···CuCl exploited two spectrometers that are each fitted with a laser ablation source.[9] Detailed descriptions of the design and operating principles of these spectrometers can be found in refs 9a and 9b. Measurements performed using a chirped-pulse Fourier transform microwave (CP-FTMW) spectrometer probe the entire 7−18.5 GHz bandwidth in a single data acquisition cycle. A Balle-Flygare Fourier transform microwave (BF-FTMW) spectrometer allows measurements of the frequencies of individual transitions with high precision.

The method used to generate metal-containing molecules is the same on both spectrometers. A gas sample is prepared to contain ∼0.5% CCl_4 and ∼0.5% of the hydrocarbon precursor in a balance of argon at a total pressure of 6 bar. The sample is pulsed into an evacuated chamber through a nozzle with an orifice diameter of 0.5 mm. It undergoes supersonic expansion, passing over the surface of a copper rod ablated by the focused beam from a Nd:YAG laser operating on the second harmonic (532 nm). Ablated copper reacts with components of the gas sample to generate the metal complex within the expanding jet. Isotopologues containing ^{63}Cu, ^{65}Cu, ^{35}Cl, and ^{37}Cl were generated from samples of Cu and CCl_4 which contain isotopes of copper and chlorine in their naturally occurring abundance ratios which are approximately 2:1 (^{63}Cu:^{65}Cu) and 3:1 (^{35}Cl:^{37}Cl), respectively. Synthetically enriched samples of $^{13}C_2H_4$, $^{13}C_2H_2$, and C_2D_2 were used to generate isotopologues containing ^{13}C and D. Following supersonic expansion of the prepared sample, a pulse of microwave radiation induces a macroscopic rotational polarization on resonance with a molecular rotational transition. The subsequent molecular emission, detected as the free induction decay (FID) of the polarization, is Fourier transformed to obtain the frequency domain spectrum. The experiment is repeated and averaged in the time domain to improve S/N. While the above series of events is common to experiments performed on each spectrometer used during this study, the bandwidths, durations, and intensities of introduced microwave pulses differ depending on whether the narrowband (BF-FTMW) or broadband (CP-FTMW) method is used.

Propagation of the molecular beam is perpendicular to the orientation of the detecting horn in the CP-FTMW spectrometer such that each transition is observed as a single peak with full-width at half-maximum (fwhm) ≅ 80 kHz. The antenna used to detect the molecular emission within the BF-FTMW spectrometer is located at the center of one mirror of the contained Fabry−Perot cavity. Molecules are introduced into the BF-FTMW spectrometer with velocities parallel to the axis of the cavity, and each molecular transition thus appears as a doublet or Doppler pair. Each of the components comprising the Doppler pair has full-width at half-maximum (fwhm) ≅ 10 kHz. Transition frequencies are calculated by taking an average over the two Doppler components. All frequency signals used by both instruments are locked to an external reference source accurate to 1 part per 10^{11}.

Ab-Initio Calculations. Geometry optimizations were performed using CCSD(T)(F12*),[10] a coupled-cluster method with single and double excitations, explicit correlation,[11] and a perturbative treatment of triple excitations.[12] An AVTZ basis set combination was used, by which we mean that the aug-cc-pVTZ basis sets[13] were used for the C and H atoms, the aug-cc- pV(T+d)Z basis set[14] for Cl, and the aug-cc-pVTZ-PP basis for Cu, in combination with the ECP-10-MDF effective core potential on Cu to account for scalar relativistic effects.[15,16] The frozen-core approximation was used throughout, and all calculations were performed using the MOLPRO package.[17] Dissociation energies at the CCSD(T)(F12*)/AVTZ level were computed using the counterpoise correction method where, for numerical stability, the CABS singles correction was not included in the correction term.

RESULTS

Observations and Spectral Assignment. It will be shown that C_2H_2···CuCl and C_2H_4···CuCl each have C_{2v} geometries in which the copper and chlorine atoms lie on the principal axis of symmetry which is also the *a*-inertial axis. The ethene or ethyne molecule coordinates via π electrons such that the midpoint of the respective C═C or C≡C bond is also located on the *a*-inertial axis within each complex. The resulting T-shaped geometry of C_2H_2···CuCl is shown in Figure 1.

A short section of the broadband spectrum measured by probing an expanding sample containing CCl_4, C_2H_2, argon, and products of the laser ablation of the copper rod is presented in Figure 2. Neither C_2H_2 nor CCl_4 possesses an electric dipole moment, and transitions within the observed spectrum do not assign directly to these precursors. Transitions of CuCl are identified at frequencies consistent with previous works, and in addition, new features are identified at regular intervals of approximately 4 GHz. Closer examination reveals that the general appearance of these features is consistent with the spectrum expected of an asymmetric rotor of asymmetry parameter that lies close to the prolate symmetric-rotor limit. Specifically, each observed $J'' \leftarrow J'$ transition consists of a central band of hyperfine components where $K_{-1} = 0$, and two further bands (respectively found at reproducible frequency increments slightly higher or lower in frequency than the central $K_{-1} = 0$ band) are yielded by transitions where $K_{-1} = 1$. The molecular carrier of the observed spectrum thus adopts a geometry in which most of the mass is located on or near to the *a*-inertial axis. All observed transitions are *a* type in character, consistent with there being a component of the electric dipole moment of the molecule aligned with the *a*-inertial axis. The intensities of transitions with $K_{-1} = 0$ relative to those of

dx.doi.org/10.1021/ic501899c | Inorg. Chem. 2014, 53, 10722−10730

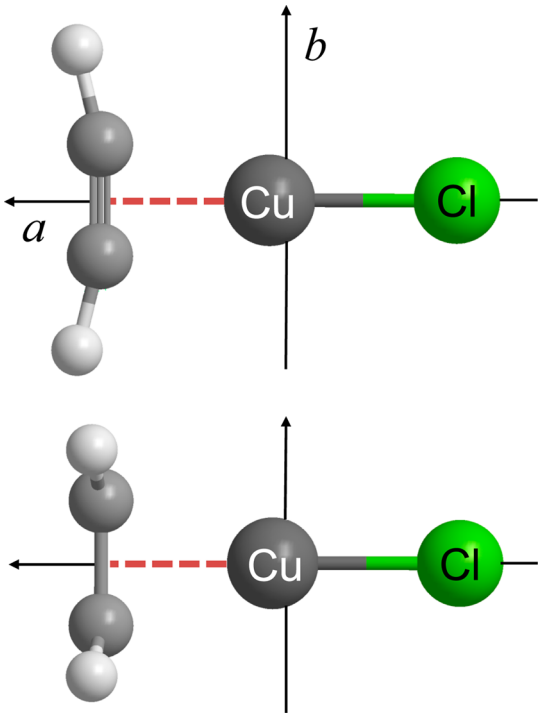

Figure 1. Structural models used to interpret the spectra of $C_2H_2\cdots$CuCl (top) and $C_2H_4\cdots$CuCl (bottom). In each case, the *a*-inertial axis is aligned with the axis defined by Cu and Cl while the *b*-inertial axis is perpendicular to it. Bond lengths and angles are to scale.

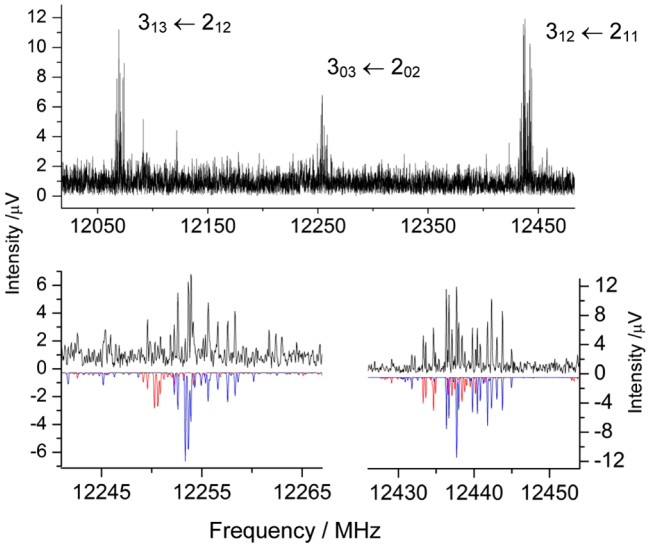

Figure 2. Section of the broadband spectrum of $C_2H_2\cdots$CuCl illustrating the $J' \leftarrow J''= 3 \leftarrow 2$ transition after approximately a million averages. As shown in the top panel, transitions where $K_{-1} = 1$ are found on either side of a central band of $K_{-1} = 0$ transitions, as expected for *a*-type transitions of a near-prolate asymmetric top. Intensities of the $K_{-1} = 0$ and $K_{-1} = 1$ transitions are consistent with the expected nuclear spin statistical weights. Bottom panels show expanded views that allow spectra simulated from the model Hamiltonian to be compared with the experimental measurement. Simulated spectra of $^{12}C_2H_2\cdots{}^{63}Cu^{35}Cl$ and $^{12}C_2H_2\cdots{}^{65}Cu^{35}Cl$ are, respectively, shown in blue and red.

transitions where $K_{-1} = 1$ imply a C_{2v} geometry for the molecular carrier. Extensive hyperfine splittings in each band imply the presence of one or more nuclei where $I > 1/2$. The initial evidence thus strongly suggested an initial, tentative assignment to a complex of $C_2H_2\cdots$CuCl of the geometry shown in Figure 1. Proof that the spectrum should be assigned to this complex will be presented (see Molecular Geometry) through the results of extensive experiments that precisely measure changes in the various rotational constants on isotopic substitution. Observed transitions of isotopologues of $C_2H_2\cdots$CuCl were remeasured at higher resolution using the BF-FTMW spectrometer prior to fits of the spectroscopic transitions (described below) to the model Hamiltonian.

The approach used to interpret the spectrum of $C_2H_4\cdots$CuCl was the same as that employed to study $C_2H_2\cdots$CuCl. Each complex is observed to yield a spectrum of similar intensity and with similar features, as expected given that each complex adopts the same fundamental geometry and contains a very similar range of nuclei. It will be shown (below) that the axis of the CuCl subunit is aligned perpendicular to the plane of the C_2H_4 subunit in $C_2H_4\cdots$CuCl. An initial survey of transitions was performed using the CP-FTMW spectrometer to probe an expanding gas sample containing C_2H_4, CCl_4, Ar, and products generated by laser ablation of the Cu rod. A key distinction between the spectra of $C_2H_4\cdots$CuCl and $C_2H_2\cdots$CuCl is a difference in the observed intensities of transitions where $K_{-1} = 1$ relative to those where $K_{-1} = 0$. It is apparent from the short section of the broadband spectrum shown in Figure 2 that the intensities of $K_{-1} = 1$ transitions of $^{12}C_2H_2\cdots{}^{63}Cu^{35}Cl$ are greater than those where $K_{-1} = 0$ by a factor of 3. This is consistent with the weighting of 3:1 expected from nuclear spin statistics when an exchange of two equivalent protons occurs by a C_2^a symmetry operation. The ratio of the intensities of $K_{-1} = 1$ and $K_{-1} = 0$ transitions expected and observed in the broadband spectrum (Figure 3) for $^{12}C_2H_4\cdots{}^{63}Cu^{35}Cl$ is 1:2.

Transitions in the observed spectra were assigned with quantum numbers and the measured frequencies fitted to model Hamiltonians using the PGOPHER program.[18] The Hamiltonians employed to describe each complex are constructed as shown below

$$H = H_R - \frac{1}{6}\mathbf{Q}(\mathrm{Cu})\colon \nabla\mathbf{E}(\mathrm{Cu}) - \frac{1}{6}\mathbf{Q}(\mathrm{Cl})\colon \nabla\mathbf{E}(\mathrm{Cl}) + \boldsymbol{I}_{\mathrm{Cu}}\cdot\mathbf{C}_{\mathrm{Cu}}\cdot\boldsymbol{J} \quad (1)$$

The rotational Hamiltonian of a semirigid asymmetric top is denoted by H_R. Details of the molecular geometry of each complex can be obtained by fitting the rotational constants, A_0, B_0, and C_0, which each contribute to H_R. These three parameters are inversely proportional to the respective moments of inertia about the inertial axes, *a*, *b*, and *c*. Centrifugal distortion of the molecular geometry also contributes to H_R. The second and third terms of eq 1 describe the nuclear quadrupole coupling interactions between the nuclear electric quadrupole moments of the respective copper and chlorine nuclei ($I = 3/2$ for each of ^{63}Cu, ^{65}Cu, ^{35}Cl, and ^{37}Cl) and the electric field gradients at each of these nuclei. The last term in eq 1 describes the magnetic coupling between the nuclear spin of the copper atom ($I = 3/2$ for each of ^{63}Cu and ^{65}Cu) and the rotation of the molecular framework.

The BF-FTMW spectrometer was employed to measure all transitions fitted for $C_2H_2\cdots$CuCl (Tables 1 and 2). The rotational constants, A_0, B_0, and C_0, were fitted to measured transition frequencies for all five isotopologues of $C_2H_2\cdots$CuCl studied. The nuclear quadrupole coupling constants, χ_{aa}(Cu),

dx.doi.org/10.1021/ic501899c | Inorg. Chem. 2014, 53, 10722−10730

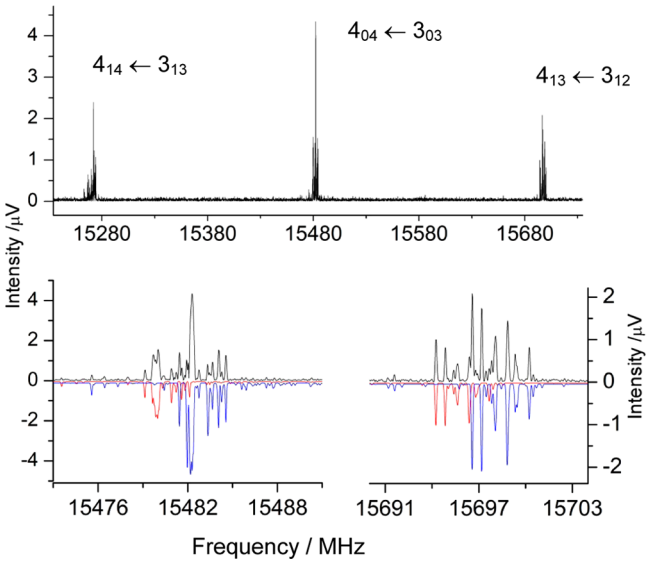

Figure 3. Section of the broadband spectrum of $C_2H_4\cdots CuCl$ illustrating the $J' \leftarrow J'' = 4 \leftarrow 3$ transition after approximately 150k averages (top). Again, transitions where $K_{-1} = 1$ and $K_{-1} = 0$ are distributed as expected for *a*-type transitions of a near-prolate asymmetric top. Relative intensities of these transitions are as expected given the nuclear spin statistical weights predicted for the $^{12}C_2H_4\cdots{}^{63}Cu^{35}Cl$ complex from the model geometry. (Bottom) Expanded views that allow spectra simulated from the model Hamiltonian to be compared with the experimental measurement. Simulated spectra of $^{12}C_2H_4\cdots{}^{63}Cu^{35}Cl$ and $^{12}C_2H_4\cdots{}^{65}Cu^{35}Cl$ are, respectively, shown in blue and red.

$[\chi_{bb}(Cu) - \chi_{cc}(Cu)]$, $\chi_{aa}(Cl)$, and $[\chi_{bb}(Cl) - \chi_{cc}(Cl)]$, representing projections of the nuclear quadrupole coupling tensors of copper and chlorine onto the respective inertial axes were also fitted for all isotopologues. The data allow the independent determination of A_0, B_0, C_0, together with three (Δ_J, Δ_{JK} and δ_J) of the five quartic centrifugal distortion constants for some but not all isotopologues. Given that centrifugal distortion constants can be calculated with high precision, a semiempirical approach was adopted toward these quantities during analysis. Values of Δ_J, Δ_{JK}, and δ_J for $^{12}C_2H_2\cdots{}^{63}Cu^{35}Cl$ were determined to be 0.270 kHz, 31.77 kHz, and 17.2 Hz at the MP2/cc-pVTZ level of theory. These calculated values were divided by those determined experimentally to determine scaling factors that connect the theoretical with experimental results for other isotopologues. For $^{12}C_2H_2\cdots{}^{63}Cu^{37}Cl$, for example, values of Δ_J, Δ_{JK}, and δ_J are calculated, multiplied by the appropriate scaling factors, and then fixed during fits of other parameters to the measured transition frequencies. An equivalent procedure is also used to determine values of δ_J that are held fixed while fitting parameters to measured transitions for $^{12}C_2H_2\cdots{}^{65}Cu^{35}Cl$, $^{12}C_2D_2\cdots{}^{63}Cu^{35}Cl$, and $^{13}C_2H_2\cdots{}^{63}Cu^{35}Cl$. The nuclear spin-rotation constants, $C_{aa}(Cu)$, $C_{bb}(Cu)$, and $C_{cc}(Cu)$, are held fixed at values determined for $^{12}C_2H_2\cdots{}^{63}Cu^{35}Cl$ in fits of data for other isotopologues. This approach allows values of A_0 to be determined for every isotopologue of $^{12}C_2H_2\cdots CuCl$, allowing significant insight into the molecular geometry of this complex.

Data fitted for the most naturally abundant isotopologues of $C_2H_4\cdots CuCl$ were measured using the CP-FTMW spectrometer (Figure 3). This instrument allowed a very high number of transitions to be measured rapidly. It was thus possible to determine highly precise values of spectroscopic parameters

Table 1. Spectroscopic Constants Determined for Isotopologues of $C_2H_2\cdots CuCl$ Containing $^{12}C_2H_2$

spectroscopic constant	$^{12}C_2H_2\cdots{}^{63}Cu^{35}Cl$	$^{12}C_2H_2\cdots{}^{63}Cu^{37}Cl$	$^{12}C_2H_2\cdots{}^{65}Cu^{35}Cl$
A_0/MHz	34 614(16)[a]	34 630(34)	34 543(128)
B_0/MHz	2103.98514(29)	2044.60911(16)	2103.43217(94)
C_0/MHz	1981.20501(25)	1928.45975(19)	1980.71468(82)
Δ_{JK}/kHz	31.24(14)	[32.54][b]	31.7(11)
Δ_J/kHz	0.2968(50)	[0.3127][b]	0.257(42)
δ_J/Hz	16.1(38)	[17.4][b]	[16.1][b]
$\chi_{aa}(Cu)$/MHz	65.3137(38)	65.346(28)	60.378(77)
$[\chi_{bb}(Cu) - \chi_{cc}(Cu)]$/MHz	−65.848(18)	−65.835(89)	−60.96(18)
$C_{aa}(Cu)$/kHz	30.9(14)	[30.9][c]	[30.9][c]
$C_{bb}(Cu)$/kHz	9.07(73)	[9.07][c]	[9.07][c]
$C_{cc}(Cu)$/kHz	7.08(50)	[7.08][c]	[7.08][c]
$\chi_{aa}(Cl)$/MHz	−21.7550(28)	−17.188(29)	−21.747(34)
$[\chi_{bb}(Cl) - \chi_{cc}(Cl)]$/MHz	−6.4101(87)	−5.183(68)	−6.15(14)
N[c]	63	25	28
σ_{rms}/kHz[d]	1.0	1.7	3.9
Δ_0/(u Å^2)[e]	0.29	0.29	0.25
k_σ/(N m^{-1})[f]	155(3)		179(30)
k_σ/(N m^{-1})[g]	87(2)		100(17)
ω/cm^{-1}[g]	267(5)		286(47)

[a]Numbers in parentheses are one standard deviation in units of the last significant figure. [b]Where indicated by square brackets, Δ_{JK} and δ_J fixed to semiempirical values calculated by scaling the results of MP2/cc-pVTZ calculations (see text) by the ratio of experimental and calculated values for each of these parameters for the $^{12}C_2H_2\cdots{}^{63}Cu^{35}Cl$ isotopologue. [c]Fixed to values determined for the most naturally abundant species, $^{12}C_2H_2\cdots{}^{63}Cu^{35}Cl$. [d]$N$ is the number of fitted spectral transitions, and σ_{rms} is the standard deviation of the fit. [e]The inertia defect where $\Delta_0 = I_c^0 - I_b^0 - I_a^0$. [f]The stretching force constant, k_σ, determined under the simple pseudodiatomic approximation.[26] [g]The stretching force constant, k_σ, is determined by Millen's method[27a] for weakly bound dimers, while the vibrational frequency of the intermolecular bond is determined from this force constant.

even though the frequency resolution of the CP-FTMW spectrometer is lower than that achieved by the BF-FTMW spectrometer with respect to measurement of individual transition frequencies. Transitions of isotopologues containing ^{13}C were recorded exclusively using the BF-FTMW spectrometer. The results of the fitting are shown in Tables 3 and 4. Values of A_0, B_0, C_0, Δ_J, Δ_{JK}, $\chi_{aa}(Cu)$, $[\chi_{bb}(Cu) - \chi_{cc}(Cu)]$, $\chi_{aa}(Cl)$, and $[\chi_{bb}(Cl) - \chi_{cc}(Cl)]$ were independently determined for the four isotopologues containing $^{12}C_2H_4$. Values for the A_0 rotational constants of $^{13}C_2H_4\cdots{}^{63}Cu^{35}Cl$ and $^{13}C_2H_4\cdots{}^{65}Cu^{35}Cl$ and B_0-C_0 of $^{13}C_2H_4\cdots{}^{65}Cu^{35}Cl$ were established from the ab-initio geometry calculated at the CCSD(T)(F12*)/AVTZ level, allowing other rotational constants to be determined for these isotopologues. The values of $\chi_{aa}(Cu)$ and $[\chi_{bb}(Cu) - \chi_{cc}(Cu)]$ for $^{13}C_2H_4\cdots{}^{63}Cu^{35}Cl$ were held fixed to the evaluated results for $^{12}C_2H_4\cdots{}^{63}Cu^{35}Cl$. For $^{13}C_2H_4\cdots{}^{65}Cu^{35}Cl$, the same quantities were fixed to the results obtained for $^{12}C_2H_4\cdots{}^{65}Cu^{35}Cl$. A low number of measured transitions and lack of data from transitions with $K_{-1} = 1$ prevent independent determination of B_0 and C_0 for $^{13}C_2H_4\cdots{}^{65}Cu^{35}Cl$. For this reason, only $(B_0 + C_0)/2$ is available for this isotopologue.

Molecular Geometries of $C_2H_2\cdots CuCl$ and $C_2H_4\cdots CuCl$. Substitution of ^{63}Cu for ^{65}Cu in each of $C_2H_2\cdots CuCl$ and

dx.doi.org/10.1021/ic501899c | Inorg. Chem. 2014, 53, 10722−10730

Table 2. Spectroscopic Constants Determined for Isotopologues of C_2H_2···CuCl Containing C_2D_2 and $^{13}C_2H_2$

spectroscopic constant	$^{12}C_2D_2$ ···$^{63}Cu^{35}Cl$	$^{13}C_2H_2$ ···$^{63}Cu^{35}Cl$
A_0/MHz	25 102(31)[a]	32 883.0(359)
B_0/MHz	2015.92453(70)	2032.35980(36)
C_0/MHz	1864.01322(73)	1912.01642(29)
Δ_{JK}/kHz	29.41(84)	28.44(35)
Δ_J/kHz	0.243(36)	0.276(14)
δ_J/Hz	[14.3][b]	[15.3][b]
χ_{aa}(Cu)/MHz	65.44(56)	65.359(24)
$[\chi_{bb}(Cu)-\chi_{cc}(Cu)]$/MHz	−65.93(41)	−65.867(62)
C_{aa}(Cu)/kHz	[30.9][c]	31.1(58)
C_{bb}(Cu)/kHz	[9.07][c]	6.8(18)
C_{cc}(Cu)/kHz	[7.08][c]	8.6(13)
χ_{aa}(Cl)/MHz	−21.765(60)	−21.7520(93)
$[\chi_{bb}(Cl)-\chi_{cc}(Cl)]$/MHz	−6.60(71)	−6.509(79)
N[c]	27	40
σ_{rms}/kHz	3.9	1.8
Δ_0/(u Å^2)	0.30	0.28
k_σ/(N m^{-1})[d]	172(25)	150(7)
k_σ/(N m^{-1})[e]	96(15)	91(4)
ω/cm^{-1}	273(41)	266(13)

[a]Numbers in parentheses are one standard deviation in units of the last significant figure. [b]Where indicated by square brackets, Δ_{JK} and δ_J fixed to semiempirical values calculated by scaling the results of MP2/cc-pVTZ calculations (see text) by the ratio of experimental and calculated values for each of these parameters for the $^{12}C_2H_2$···$^{63}Cu^{35}Cl$ isotopologue. [c]Fixed to values determined for the most naturally abundant species, $^{12}C_2H_2$···$^{63}Cu^{35}Cl$. [d]The stretching force constant, k_σ, determined under the simple pseudo-diatomic approximation.[26] [e]The stretching force constant, k_σ, is determined by Millen's method[27a] for weakly bound dimers, while the vibrational frequency of the intermolecular bond is determined from this force constant.

Table 4. Spectroscopic Constants of Isotopologues of C_2H_4···CuCl Containing ^{13}C

spectroscopic constant	$^{13}C_2H_4$ ···$^{63}Cu^{35}Cl$	$^{13}C_2H_4$ ···$^{65}Cu^{35}Cl$
A_0/MHz	[23 068][a]	[23 068][a]
B_0/MHz	1925.9798(490)[b]	
C_0/MHz	1819.6292(478)	
$[(B_0 + C_0)/2]$/MHz		1872.64544(31)[c]
Δ_{JK}/kHz	[18.02][d]	[18.04][d]
Δ_J/kHz	[0.250][d]	[0.250][d]
χ_{aa}(Cu)/MHz	[63.778][e]	[59.058][f]
$[\chi_{bb}(Cu) - \chi_{cc}(Cu)]$/MHz	[−44.52][e]	[−41.39][f]
χ_{aa}(Cl)/MHz	[−20.99][e]	[−20.992][f]
$[\chi_{bb}(Cl) - \chi_{cc}(Cl)]$/MHz	[−5.09][e]	[−4.97][f]
N[g]	12	7
σ_{rms}/kHz[g]	4.6	4.9

[a]A_0 fixed to the value of 23 068 MHz calculated for this parameter at the CCSD(T)(F12*)/AVTZ level. [b]Numbers in parentheses are one standard deviation in units of the last significant figure. [c]$B_0 - C_0$ fixed to the value of 106.30871 MHz, which is calculated (at the CCSD(T)(F12*)/AVTZ level) to be the difference between the equilibrium values of B and C. [d]Δ_{JK} and Δ_J fixed to semiempirical values calculated by scaling the results of MP2/cc-pVTZ calculations (see text) by the ratio of the experimental and calculated values for $^{12}C_2H_4$···$^{63}Cu^{35}Cl$. [e]Fixed to the result obtained for $^{12}C_2H_4$···$^{63}Cu^{35}Cl$. [f]Fixed to the result obtained for $^{12}C_2H_4$···$^{65}Cu^{35}Cl$. [g]N is the number of fitted spectral transitions and σ_{rms} is the standard deviation of the fit.

C_2H_4···CuCl (for any given combination of H, C, and Cl isotopes) induces only a small change in the measured rotational constants, implying that the copper atom is close to the center of mass in each complex studied. Evidence in support of a planar geometry for C_2H_2···CuCl is provided by the calculated inertia defects, Δ_0

$$\Delta_0 = I_c^0 - I_a^0 - I_b^0 \quad (2)$$

Table 3. Spectroscopic Constants Determined for Four Isotopologues of C_2H_4···CuCl

spectroscopic constant	$^{12}C_2H_4$···$^{63}Cu^{35}Cl$	$^{12}C_2H_4$ ···$^{65}Cu^{35}Cl$	$^{12}C_2H_4$ ···$^{63}Cu^{37}Cl$	$^{12}C_2H_4$ ···$^{65}Cu^{37}Cl$
A_0/MHz	23 911(56)[a,b]	24 220(60)	24 034(99)	23 793(115)
B_0/MHz	1988.93172(62)	1988.62176(64)	1933.70910(77)	1933.2820(11)
C_0/MHz	1882.69424(62)	1882.41548(65)	1833.13167(79)	1832.7466(11)
Δ_{JK}/kHz	19.49(83)	15.59(89)	16.8(14)	22.33(172)
Δ_J/kHz	0.266(31)	0.386(32)	0.2656(531)	0.1750(569)
χ_{aa}(Cu)/MHz	63.7777(90)	59.058(37)	63.859(16)	59.173(68)
$[\chi_{bb}(Cu) - \chi_{cc}(Cu)]$/MHz	−44.521(30)	−41.39(20)	−44.69(17)	−41.60(23)
χ_{aa}(Cl)/MHz	−20.992(13)	−20.992(19)	−16.567(16)	−16.577(49)
$[\chi_{bb}(Cl) - \chi_{cc}(Cl)]$/MHz	−5.093(39)	−4.97(33)	−3.95(13)	−3.98(15)
N	166	94	77	46
σ_{rms}/kHz	10.3	8.0	8.6	6.9
Δ_0/(u Å^2)	0.19[c]	0.30[c]	0.46[c]	0.08[c]
P_b/(u Å^2)	17.74(4)[d]	17.68(7)	17.60(4)	17.79(9)
P_c/(u Å^2)	3.399(8)[d]	3.34(1)	3.264(8)	3.45(2)
k_σ/(N m^{-1})[f]	156(18)	144(29)	108(9)	220(72)
k_σ/(N m^{-1})[g]	88(10)	61(5)	82(16)	124(40)
ω/cm^{-1} [g]	262(30)	217(18)	252(50)	309(101)

[a]Numbers in parentheses are one standard deviation in units of the last significant figure. [b]The rotational constants A_0, B_0, and C_0 of isolated C_2H_4 are 14 5837.8, 30 010.91, and 24 824.20 MHz, respectively. [c]Δ_0 is the pseudoinertia defect determined by subtracting the contribution of the four hydrogen atoms from $I_c^0 - I_b^0 - I_a^0$ of C_2H_4···CuCl. [d]The planar moments of isolated C_2H_4 are P_a^E =16.8664, P_b^E =3.4919, and P_c^E = −0.02656 u Å^2, respectively. [f]The stretching force constant, k_σ, determined under the simple pseudodiatomic approximation.[26] [g]The stretching force constant, k_σ, is determined by Millen's method[27a] for weakly bound dimers, while the vibrational frequency of the intermolecular bond is determined from this force constant.

dx.doi.org/10.1021/ic501899c | Inorg. Chem. 2014, 53, 10722−10730

where I_a^0, I_b^0, and I_c^0 are the moments of inertia determined from the experimentally measured A_0, B_0, and C_0 rotational constants. The inertia defects of isotopologues of $C_2H_2\cdots$CuCl range from 0.25 to 0.30 u Å^2 with the average being 0.28(1) u Å^2, consistent with the small and positive result expected for a planar molecule. The inertia defects of $C_2H_2\cdots$HCl, $C_2H_2\cdots$ClF, $C_2H_2\cdots$AgCCH, and $C_2H_2\cdots$AgCl are 1.2(3), 0.636(2), 0.38(5), and 0.34(3) u Å^2, respectively. The trend in this series indicates an increase in the stiffness of the intermolecular bond.[7k,8,19,20] It is possible to calculate a pseudoinertial defect for $C_2H_4\cdots$CuCl on the assumption that the carbon, copper, and chlorine atoms of $C_2H_4\cdots$CuCl are all coplanar while the H atoms lie outside the plane defined by the heavier atoms. Under this assumption, the contributions of the H atoms can be removed from the inertia defect as defined in eq 2 by addition of $8m_H(b_H^E)^2$, where m_H is the mass of a hydrogen atom and b_H^E is the b coordinate of a single hydrogen atom in the free ethene molecule. The results are values of Δ_0 = 0.19(3), 0.30(9), 0.46(4), and 0.08(6) u Å^2 for $^{12}C_2H_4\cdots{}^{63}Cu^{35}Cl$, $^{12}C_2H_4\cdots{}^{65}Cu^{35}Cl$, $^{12}C_2H_4\cdots{}^{63}Cu^{37}Cl$, and $^{12}C_2H_4\cdots{}^{65}Cu^{37}Cl$, respectively, consistent with the original assumption that the Cu, Cl, and C atoms lie within the same plane.

Further evidence for the C_{2v} geometry of $C_2H_4\cdots$CuCl is available from the evaluated planar moments of this complex. These are defined as

$$P_\alpha = \frac{1}{2}(-I_\alpha + I_\beta + I_\gamma) \tag{3}$$

where α, β, and γ are permuted cyclically over the three inertial axes. For a complex of $C_2H_4\cdots$CuCl in the described C_{2v} geometry, the equilibrium values of P_b and P_c can be expected to be similar to P_a^E = 16.8664 and P_b^E = 3.4919 u Å^2, which are, respectively, the planar moments about the a and b axes of free C_2H_4. Taking an average over the results for the various isotopologues of the complex, P_b is 17.70(6) u Å^2 and P_c is 3.36(1) u Å^2. These results are similar to the aforementioned values of P_a^E and P_b^E for isolated C_2H_4.[21] The results thus confirm C_{2v} geometries for both $C_2H_2\cdots$CuCl and $C_2H_4\cdots$CuCl. While the former is planar, the latter has carbon, copper, and chlorine atoms all lying within the same plane. The axis of the CuCl subunit is oriented perpendicular to the plane of the C_2H_4 subunit in the model geometry. However, it is also important to note that despite the similarity between the results obtained for P_b of $C_2H_4\cdots$CuCl and P_a^E the former is greater than the latter by a small but significant amount. This result implies a slight change in the geometry of the C_2H_4 subunit on formation of the complex. This possibility is now explored further through fitting of the r_0 geometries of both complexes to experimentally determined moments of inertia using the STRFIT program of Kisiel.[22]

The geometry can be determined most comprehensively for $C_2H_2\cdots$CuCl, where there are fewer geometrical parameters, data is available from deuterated isotopologues, and there are a greater number of precisely determined rotational constants available. Given that isotopic substitutions are possible at the C, H, Cu, and Cl atoms, r(C≡C), r(*···Cu), r(Cu−Cl) and, in principle, r(C−H) can be precisely determined from the data. Simultaneous fitting of r(C−H) and ∠(*−C−H) gives correlated results for these parameters, however. An alternative approach, previously adopted during recent studies of $C_2H_2\cdots$AgCl and $C_2H_2\cdots$AgCCH, involves fixing r(C−H) at the value calculated ab initio (after applying a small correction for the expected differences between the r_e and r_0 geometries) and fitting ∠(*−C−H) to the experimental data. This procedure yields the geometry shown in Table 5. The most striking change from the free molecules entails a distortion of the linear geometry of the ethyne subunit such that the hydrogen atoms move away from the copper atom within the complex. Measured values of the A_0, B_0, and C_0 rotational constants are available for four isotopologues of $C_2H_4\cdots$CuCl. Only B_0 and C_0 were independently measured for $^{13}C_2H_4\cdots{}^{63}Cu^{35}Cl$, and only $(B_0 + C_0)/2$ is available for $^{13}C_2H_4\cdots{}^{65}Cu^{35}Cl$. Given that it is not possible to simultaneously determine the r(C−H) bond length, the ∠(*−C−H) angle, and the ∠(HCCCu) dihedral angle in the absence of data from deuterated isotopologues, the first is fixed at the r_e value calculated at the CCSD(T)(F12*)/AVTZ level after applying a small correction for the difference between the r_e and the r_0 values of this parameter in the free C_2H_4 molecule. The ∠(HCCCu) dihedral angle is fixed at the r_e value calculated at the CCSD(T)(F12*)/AVTZ level to allow determination of the r_0 parameters shown in Table 6. Again, the geometry of the hydrocarbon subunit changes such that the hydrogen atoms move away from the copper atom.

Table 5. Geometries of $C_2H_2\cdots$CuCl and Isolated C_2H_2

	$C_2H_2\cdots$CuCl		
	r_s (exp.)	r_0 (exp.)	r_e (CCSD(T)(F12*) AVTZ)
r(*−Cu)/Å	1.887(2)[a]	1.888(15)	1.872
r(Cu−Cl)/Å	2.069(2)	2.071(12)	2.062
r(C≡C)/Å	1.238(4)	1.2334(25)	1.232
r(C−H)/Å	[1.072][b]	[1.072][b]	1.069
∠(*−C−H)/°	192.5(2)	192.4(7)	193.1
a_{Cu}/Å	0.179(8)	0.184(5)	0.191
a_{Cu}/Å (first mom.)	0.184(1)		
a_{Cl}/Å	−1.8848(8)	−1.886(7)	−1.871
$a^* = a_C$/Å	2.0705(7)	2.072(9)	2.063
b_C/Å	±0.619(2)	±0.6163(12)	±0.616
a_H/Å	2.3018(7)	2.302(9)	2.305
b_H/Å	±1.6580(9)	±1.663(13)	±1.657
	C_2H_2		
	r_0 (exp.)[c]	r_e (exp.)[d]	r_e (CCSD(T)(F12*)AVTZ)[e]
r(C≡C)/Å	1.206553(6)	1.20286(3)	1.2055
r(C−H)/Å	1.06238(2)	1.06166(6)	1.0631
	$^{12}C_2H_2$	$^{13}C_2H_2$	C_2D_2
B_0/MHz	35 274.9693(54)[c]	33 564.005[c]	25 418.6291[c]

[a]Numbers in parentheses are one standard deviation in units of the last significant figure. [b]Fixed to the value obtained by correcting the r_e result calculated at the CCSD(T)(F12*)/AVTZ level for the difference between the experimentally measured r_0 and r_e distances of C_2H_2. [c]Reference 35. [d]Reference 36. [e]This work.

An alternative method employs measured changes in the moments of inertia on isotopic substitution to calculate the coordinates of substituted atoms.[23] The a coordinate of an atom, Y, located on the a axis is given by

$$\left\{\frac{\Delta I_b + \Delta I_c}{2\mu_s}\right\}^{1/2} = |a_Y| \tag{4}$$

where ΔI_b and ΔI_c are the changes in the moments of inertia on isotopic substitution of atom Y where $\mu_s = ((\Delta mM)/(M +$

dx.doi.org/10.1021/ic501899c | Inorg. Chem. 2014, 53, 10722−10730

Table 6. Geometries of C_2H_4···CuCl and Isolated C_2H_4

	C_2H_4···CuCl		
	r_s (exp.)	r_0 (exp.)	r_e (CCSD(T)(F12*) AVTZ)
r(*−Cu)/Å	1.908(12)[a]	1.908(7)	1.895
r(Cu−Cl)/Å	2.064(8)	2.070(6)	2.063
r(C═C)/Å		1.367(3)	1.371
r(C−H)/Å		[1.088][b]	1.084
∠(*−C−H)/°		122.5(5)	121.1
∠(HCCCu)/°		[96.05]	96.05
a_{Cu}/Å	0.142(11)	0.147(3)	0.154
a_{Cl}/Å	−1.9219(8)	−1.923(3)	−1.909
$a^* = a_C$/Å	2.0505(7)	2.055(4)	2.049
b_C/Å		±0.684(1)	±0.686
a_H/Å		2.152(4)	2.147
b_H/Å		±1.269(8)	±1.245
c_H/Å		±0.913(5)	±0.923
	C_2H_4		
	r_0 (exp.)[c]	r_e (CCSD(T)(F12*) AVTZ)[d]	
r(C═C)/Å	1.3386(14)	1.3335	
r(C−H)/Å	1.0849(13)	1.0823	
∠(C═C−H)/°	121.16(11)	121.42	

[a]Numbers in parentheses are one standard deviation in units of the last significant figure. [b]Fixed to the value obtained by correcting the r_e result calculated at the CCSD(T)(F12*)/AVTZ level for the difference between the experimentally measured r_0 and r_e distances of C_2H_4. [c]Calculated by fitting the principal moments of inertia of $^{12}C_2H_4$, $^{12}CH_2{}^{12}CHD$, $^{12}CH_2{}^{12}CD_2$, $^{12}CHD{}^{12}CHD$, and $^{13}CH_2{}^{12}CH_2$ from ref 21 and those of $^{12}C_2H_4$ from ref 30. [d]This work.

Δm)) is the reduced mass arising from a mass change, Δm, in a parent isotopologue of mass, M. Similar expressions use the measured shifts on double substitution to calculate the a and b coordinates of atoms that do not lie on the a axis but which are interchanged by a C_2 rotation.[24] The range of isotopic substitutions performed during this work allows a nearly complete r_s geometry to be provided for C_2H_2···CuCl with the evaluated parameters highly consistent with the r_0 results. Data available for C_2H_4···CuCl are more limited. Substitutions are not available at the H atoms, and A_0 rotational constants are not available for isotopologues containing ^{13}C. As a consequence, r_s values can be provided only for the a coordinates of the carbon, copper, and chlorine atoms. Although the r_s method does not explicitly provide the sign of coordinates, only the assignments listed in Tables 5 and 6 yield results that are physically realistic for each complex. Uncertainties in r_s parameters are greatest with respect to small coordinates, so large uncertainties are associated with the location of the copper atom in each case. An alternative approach to the calculation of small coordinates[25] uses the first moment condition ($a_{Cu} = (-\sum_j a_j m_j)/m_{Cu}$) to determine the a-axis coordinate of the copper atom from knowledge of the coordinates of other atoms. Application of this method yields a value of a_{Cu} (first mom.) = 0.184(1) Å, in good agreement with the r_0 result. The value of a_{Cu} (first mom.) is therefore used to calculate r(*−Cu) and r(Cu−Cl) for the r_s geometry shown. The results of all fits to the experimentally measured rotational constants are displayed in Tables 5 and 6 alongside those of the ab-initio calculations at the CCSD(T)(F12*)/AVTZ level.

Force Constants and Nuclear Quadrupole Coupling Constants. The evaluated inertia defects imply bonds between C_2H_2/C_2H_4 and copper that are of similar strength to those in the analogous B···AgCl complexes. It is possible to estimate the force constant of each bond by making the approximation that each complex is a pseudodiatomic molecule[26] in which the C_2H_2/C_2H_4 and CuCl subunits can each be represented as point masses (Tables 1−3). A more sophisticated model provided by Millen[27] takes into account the internal structure of each of the subunits and is expressed in terms of the various rotational and centrifugal distortion constants

$$k_\sigma = (8\pi^2\mu/\Delta_J)\left[B^3(1-b) + C^3(1-c) + \frac{1}{4}(B-C)^2(B+C)(2-b-c)\right] \quad (5)$$

where $\mu = (m_{C_2H_2} m_{CuCl})/(m_{C_2H_2} + m_{CuCl})$, $b = (B/B_{C_2H_2}) + (B/B_{CuCl})$, and $c = (C/B_{C_2H_2}) + (C/B_{CuCl})$, where $B_{iC_2H_2}$ and B_{CuCl} are rotational constants of the component molecules and strictly should be equilibrium values and the spectroscopic constants B, C, and Δ_J of C_2H_2···CuCl should also be equilibrium values. Usually zero-point values are used, given that equilibrium quantities are rarely available. Equation 5 applies only in the quadratic approximation and only if the intermolecular stretching mode σ lies much lower in wavenumber than other modes of the same symmetry.

Table 7. Nuclear Quadrupole Coupling Constants and Ionicities Measured for a Range of B···MX Molecules

	B···CuCl			B···AgCl	
	χ_{aa} (^{63}Cu)[a]/MHz	χ_{aa} (^{35}Cl)/MHz	ionicity[b] of Cu−Cl	χ_{aa} (^{35}Cl)/MHz	ionicity of Ag−Cl
MCl[c]	16.2	−32.2	0.71	−36.4	0.67
Ar···MCl[d]	33.2	−28.0	0.74	−34.5	0.69
Kr···MCl[e]	36.5	−27.3	0.75	−33.8	0.69
Xe···MCl[f]	41.8	−26.1	0.76	−32.3	0.71
H_2O···MCl[g]	50.3	−25.5	0.77	−32.3	0.71
H_3N···MCl[h]				−29.8	0.73
H_2S···MCl[i]	61.8	−23.0	0.79	−29.4	0.73
C_2H_4···MCl[j]	63.8	−21.0	0.81	−27.9	0.75
C_2H_2···MCl[k]	65.3	−21.8	0.80	−28.9	0.74
OC···MCl[l]	70.8	−21.5	0.80	−28.1	0.74

[a]Uncertainties in the quoted values are much lower than the final significant figure given. [b]Ionicities calculated from χ_{aa}(Cl) values according to the Townes−Dailey model (see text). [c]References 28 and 37. [d]References 28 and 37b. [e]References 37c and 38. [f]References 29 and 39. [g]References 7f and 7i. [h]Reference 40. [i]References 7f and 41. [j]This work and ref 7g. [k]This work and ref 7k. [l]References 7d and 42.

dx.doi.org/10.1021/ic501899c | Inorg. Chem. 2014, 53, 10722−10730

Calculation of k_σ thus requires B_0, C_0, and Δ_J to be independently determined from the experimental data. These results are available for four isotopologues of each of C_2H_2···CuCl and C_2H_4···CuCl. The average of results for C_2H_2···CuCl is 94(12) N m^{-1}, while that for C_2H_4···CuCl is 77(11) N m^{-1}, implying wavenumbers for the intermolecular stretching vibrations of ω/c = 273(32) and 244(35) cm^{-1}, respectively. The result for $^{12}C_2H_4$···$^{63}Cu^{37}Cl$ is excluded from calculation of the averaged results for C_2H_4···CuCl because of the high uncertainty associated with its centrifugal distortion constant. The force constants are slightly higher than the results for C_2H_2···AgCl and C_2H_4···AgCl, which were 51(3) and 56(2) N m^{-1}, respectively. The nuclear quadrupole coupling constants measured during this work can be interpreted to provide insight into the degree of charge rearrangement that accompanies attachment of C_2H_2 or C_2H_4 to CuCl. Table 7 provides a summary of χ_{aa}(Cu) and χ_{aa}(Cl) measured for a range of B···CuCl complexes. Attachment of argon induces only a very small change in these quantities relative to their values in free CuCl.[28] Formation of stronger intermolecular bonds such as those involving Xe[29] or H_2O[7i] and CuCl is accompanied by significantly greater changes in the electric field gradients at the Cu and Cl nuclei. The changes in χ_{aa}(Cu) and χ_{aa}(Cl) on attachment of C_2H_2 or C_2H_4 to CuCl are comparable with those seen on formation of the OC···CuCl complex and among the greatest observed to date. The χ_{aa}(Cl) values can be related to the ionicities of the Cu−Cl bond in the various complexes according to the Townes−Dailey[7i] model

$$i_c = 1 + \frac{\chi_{aa}(X)}{eQq_{(n,l,0)}(X)} \quad (6)$$

where $eQq_{(n,l,0)}$(X) is the coupling constant that would result from a single np_z electron in the isolated chlorine atom and is 109.74 MHz.[26] The result for C_2H_2···CuCl is 0.80, while that for C_2H_4···CuCl is 0.81. The trend in the nuclear quadrupole coupling constants and ionicities of B···CuCl complexes mirrors the trend observed for B···AgCl complexes, but the fractional changes are greater in the B···CuCl complexes.

CONCLUSIONS

The most significant results of this study are provided by detailed analyses of the geometries of C_2H_2···CuCl and C_2H_4···CuCl. It has been shown that C_2H_2 and C_2H_4 each bind to the copper atom through π electrons to form complexes of C_{2v} geometry. While C_2H_2···CuCl is planar and T-shaped, the CuCl subunit is aligned with the *a*-inertial axis in C_2H_4···CuCl such that the Cu atom is equidistant from all H atoms.

It is of particular interest to note changes in the geometries of C_2H_2 and C_2H_4 on their coordination to the copper atom of each complex. The observed changes are somewhat greater than those recently observed on attachment of C_2H_2/C_2H_4 to either AgCl[7g,k] or AgCCH.[8] The r(C≡C) distance in C_2H_2 is observed to increase by 0.027 Å on formation of C_2H_2···CuCl. The ∠(*−C−H) angle is 192.4(7)°, requiring a significant change from the linear geometry of free C_2H_2. The experimental findings are consistent with the results of calculations at the CCSD(T)(F12*)/AVTZ level. The results for C_2H_4···CuCl reveal an increase of 0.029 Å in the r(C═C) distance on formation of the complex from the isolated C_2H_4 and CuCl subunits. The CCSD(T)(F12*)/AVTZ calculations predict a dihedral ∠(HCCCu) angle of 96.05°, implying a considerable change from the planar geometry of free C_2H_4.[21,30] Although the experimental observations are consistent with such a deviation from planarity of C_2H_4, it is not possible to independently quantify this change from the available experimental data. The changes in the geometries of C_2H_2 and C_2H_4 on complex formation are accompanied by slight increases in r(Cu−Cl) relative to the bond length in free CuCl.[31] The values of r(Cu−Cl) are 2.071(12) and 2.070(6) Å in C_2H_2···CuCl and C_2H_4···CuCl, respectively, whereas the r_0 bond length in the free CuCl molecule is 2.054 Å.

It is interesting to note that both C_2H_2···CuCl and C_2H_4···CuCl adopt the basic geometries predicted by some empirical rules originally suggested by Legon and Millen.[32] These rules have been widely applied to rationalize the geometries of hydrogen- and halogen-bonded complexes but have also been applied to a range of metal-containing units in recent years. These state that in the absence of a nonbonding pair on a Lewis base, B, the axis of an MX subunit (where MX is a Lewis acid) in a complex of the general form B···MX intersects the internuclear axis of atoms that form a π bond and is perpendicular to the [nodal] plane of the π orbital. The force constants of bonds separating the molecular subunits in C_2H_2···CuCl and C_2H_4···CuCl are 94(12) and 77(11) N m^{-1}, respectively. These results imply stronger bonds than found in C_2H_2···AgCl[7k] and C_2H_4···AgCl[7g] (where k_σ = 51(3) and 56(2) N m^{-1}, respectively). The typical force constants of bonds within hydrogen- and halogen-bonded complexes are significantly weaker than any of the above. For example, k_σ = 12.2 N m^{-1} for C_2H_2···ICl,[19] k_σ = 9.4 N m^{-1} for C_2H_2···BrCl,[33] and k_σ = 5.5 N m^{-1} for C_2H_2···HBr.[34] The dissociation energies (counterpoise corrected) of C_2H_2···CuCl and C_2H_4···CuCl are calculated to be 148 and 155 kJ mol^{-1}, confirming that the interactions between CuCl and each of these hydrocarbons are very strong compared with typical van der Waals-, hydrogen-, and halogen-bonded interactions. It is satisfying to note that the empirical rules originally developed to rationalize the geometries of hydrogen- and halogen-bonded complexes are evidently suitable for describing the geometries of complexes containing both copper and silver.

ASSOCIATED CONTENT

Supporting Information

Fits of all spectroscopic parameters to measured transition frequencies. This material is available free of charge via the Internet at http://pubs.acs.org.

AUTHOR INFORMATION

Corresponding Authors

*E-mail: nick.walker@newcastle.ac.uk.
*E-mail: a.c.legon@bristol.ac.uk.

Notes

The authors declare no competing financial interest.

ACKNOWLEDGMENTS

We thank the European Research Council for a postdoctoral fellowship awarded to S.L.S. and for project funding (CPFTMW-307000). Also, the Leverhulme Trust for an Emeritus Fellowship and the University of Bristol for a Senior Research Fellowship awarded to A.C.L. The award of a Ph.D. studentship to D.M.B. by the School of Chemistry of Newcastle University is gratefully acknowledged. D.P.T. thanks the Royal Society for a University Research Fellowship. W.M acknowledges the award of a Marie Curie Fellowship (IIF-301616).

REFERENCES

(1) Schroeter, K.; Schalley, C. A.; Wesendrup, R.; Schröder, D.; Schwarz, H. *Organometallics* **1997**, *16* (5), 986−994.
(2) Judai, K.; Worz, A. S.; Abbet, S.; Antonietti, J.-M.; Heiz, U.; Del Vitto, A.; Giordano, L.; Pacchioni, G. *Phys. Chem. Chem. Phys.* **2005**, *7* (5), 955−962.
(3) Molnár, Á.; Sárkány, A.; Varga, M. *J. Mol. Catal. A: Chem.* **2001**, *173* (1−2), 185−221.
(4) (a) France, M. R.; Pullins, S. H.; Duncan, M. A. *J. Chem. Phys.* **1998**, *109* (20), 8842−8850. (b) France, M. R.; Pullins, S. H.; Duncan, M. A. *J. Chem. Phys.* **1998**, *108* (17), 7049−7051. (c) Reddic, J. E.; Duncan, M. A. *Chem. Phys. Lett.* **1999**, *312* (2−4), 96−100.
(5) Kleiber, L.; Fink, H.; Niessner, R.; Panne, U. *Anal. Bioanal. Chem.* **2002**, *374* (1), 109−114.
(6) Walters, R. S.; Schleyer, P. v. R.; Corminboeuf, C.; Duncan, M. A. *J. Am. Chem. Soc.* **2005**, *127* (4), 1100−1101.
(7) (a) Frohman, D. J.; Grubbs, G. S.; Yu, Z. H.; Novick, S. E. *Inorg. Chem.* **2013**, *52* (2), 816−822. (b) Francis, S. G.; Matthews, S. L.; Poleshchuk, O. K.; Walker, N. R.; Legon, A. C. *Angew. Chem., Int. Ed.* **2006**, *45* (38), 6341−6343. (c) Walker, N. R.; Francis, S. G.; Matthews, S. L.; Rowlands, J. J.; Legon, A. C. *Mol. Phys.* **2007**, *105* (5−7), 861−869. (d) Walker, N. R.; Gerry, M. C. L. *Inorg. Chem.* **2001**, *40* (24), 6158−6166. (e) Walker, N. R.; Gerry, M. C. L. *Inorg. Chem.* **2002**, *41* (5), 1236−1244. (f) Harris, S. J.; Legon, A. C.; Walker, N. R.; Wheatley, D. E. *Angew. Chem., Int. Ed.* **2010**, *49* (1), 181−183. (g) Stephens, S. L.; Tew, D. P.; Mikhailov, V. A.; Walker, N. R.; Legon, A. C. *J. Chem. Phys.* **2011**, *135* (2), 024315. (h) Stephens, S. L.; Tew, D. P.; Walker, N. R.; Legon, A. C. *J. Mol. Spectrosc.* **2011**, *267* (1−2), 163−168. (i) Mikhailov, V. A.; Roberts, F. J.; Stephens, S. L.; Harris, S. J.; Tew, D. P.; Harvey, J. N.; Walker, N. R.; Legon, A. C. *J. Chem. Phys.* **2011**, *134* (13), 134305. (j) Riaz, S. Z.; Stephens, S. L.; Mizukami, W.; Tew, D. P.; Walker, N. R.; Legon, A. C. *Chem. Phys. Lett.* **2012**, *531*, 1−5. (k) Stephens, S. L.; Mizukami, W.; Tew, D. P.; Walker, N. R.; Legon, A. C. *J. Chem. Phys.* **2012**, *137* (17), 174302.
(8) Stephens, S. L.; Zaleski, D. P.; Mizukami, W.; Tew, D. P.; Walker, N. R.; Legon, A. C. *J. Chem. Phys.* **2014**, *140* (12), 124310.
(9) (a) Batten, S. G.; Legon, A. C. *Chem. Phys. Lett.* **2006**, *422* (1−3), 192−197. (b) Stephens, S. L.; Mizukami, W.; Tew, D. P.; Walker, N. R.; Legon, A. C. *J. Chem. Phys.* **2012**, *136* (6), 064306.
(10) Hättig, C.; Tew, D. P.; Köhn, A. *J. Chem. Phys.* **2010**, *132* (23), 231102.
(11) Hättig, C.; Klopper, W.; Köhn, A.; Tew, D. P. *Chem. Rev.* **2011**, *112* (1), 4−74.
(12) Raghavachari, K.; Trucks, G. W.; Pople, J. A.; Head-Gordon, M. *Chem. Phys. Lett.* **1989**, *157* (6), 479−483.
(13) Kendall, R. A.; Dunning, T. H.; Harrison, R. J. *J. Chem. Phys.* **1992**, *96* (9), 6796−6806.
(14) Dunning, T. H.; Peterson, K. A.; Wilson, A. K. *J. Chem. Phys.* **2001**, *114* (21), 9244−9253.
(15) Peterson, K. A.; Puzzarini, C. *Theor. Chem. Acc.* **2005**, *114* (4−5), 283−296.
(16) Dolg, M.; Wedig, U.; Stoll, H.; Preuss, H. *J. Chem. Phys.* **1987**, *86* (2), 866−872.
(17) Werner, H.-J.; P. J. K, Lindh, R.; Manby, F. R.; Schütz, M. *MOLPRO*, version 2009.1, a package of ab initio programs; 2009; see http://www.molpro.net.
(18) Western, C. M. *PGOPHER, a program for simulating rotational structure*, version 6.0.202; University of Bristol: 2010; see http://pgopher.chm.bris.ac.uk for more detail about PGOPHER.
(19) Legon, A. C.; Aldrich, P. D.; Flygare, W. H. *J. Chem. Phys.* **1981**, *75* (2), 625−630.
(20) Bloemink, H. I.; Hinds, K.; Legon, A. C.; Holloway, J. H. *J. Chem. Soc., Chem. Commun.* **1995**, No. 18, 1833−1834.
(21) Craig, N. C.; Groner, P.; McKean, D. C. *J. Phys. Chem. A* **2006**, *110* (23), 7461−7469.
(22) Kisiel, Z. *J. Mol. Spectrosc.* **2003**, *218* (1), 58−67.
(23) Kraitchman, J. *Am. J. Phys.* **1953**, *21* (1), 17−24.
(24) Chutjian, A. *J. Mol. Spectrosc.* **1964**, *14* (1−4), 361−370.
(25) Costain, C. C. *J. Chem. Phys.* **1958**, *29*, 864.
(26) Gordy, W.; Cook, R. L. *Microwave molecular spectra*; Wiley: New York, 1984.
(27) (a) Millen, D. J. *Can. J. Chem.* **1985**, *63* (7), 1477−1479. (b) Read, W. G.; Campbell, E. J.; Henderson, G. *J. Chem. Phys.* **1983**, *78* (6), 3501−3508.
(28) Evans, C. J.; Gerry, M. C. L. *J. Chem. Phys.* **2000**, *112* (21), 9363−9374.
(29) Michaud, J. M.; Gerry, M. C. L. *J. Am. Chem. Soc.* **2006**, *128* (23), 7613−7621.
(30) Tan, T. L.; Goh, K. L.; Ong, P. P.; Teo, H. H. *J. Mol. Spectrosc.* **2001**, *207* (2), 189−192.
(31) Low, R. J.; Varberg, T. D.; Connelly, J. P.; Auty, A. R.; Howard, B. J.; Brown, J. M. *J. Mol. Spectrosc.* **1993**, *161* (2), 499−510.
(32) (a) Legon, A. C.; Millen, D. J. *Faraday Discuss.* **1982**, *73*, 71−87. (b) Legon, A. C. *Angew. Chem., Int. Ed.* **1999**, *38* (18), 2686−2714.
(33) Bloemink, H. I.; Hinds, K.; Legon, A. C.; Thorn, J. C. *J. Chem. Soc., Chem. Commun.* **1994**, *10*, 1229−1230.
(34) Cole, G. C.; Davey, J. B.; Legon, A. C.; Lyndon, A. F. *Mol. Phys.* **2003**, *101* (4−5), 603−612.
(35) Herman, M.; Campargue, A.; El Idrissi, M. I.; Vander Auwera, J. *J. Phys. Chem. Ref. Data* **2003**, *32* (3), 921−1361.
(36) Lievin, J.; Demaison, J.; Herman, M.; Fayt, A.; Puzzarini, C. *J. Chem. Phys.* **2011**, *134* (6), 064119.
(37) (a) Hensel, K. D.; Styger, C.; Jäger, W.; Merer, A. J.; Gerry, M. C. L. *J. Chem. Phys.* **1993**, *99* (5), 3320−3328. (b) Evans, C. J.; Gerry, M. C. L. *J. Chem. Phys.* **2000**, *112* (3), 1321−1329. (c) Michaud, J. M.; Cooke, S. A.; Gerry, M. C. L. *Inorg. Chem.* **2004**, *43* (13), 3871−3881.
(38) Reynard, L. M.; Evans, C. J.; Gerry, M. C. L. *J. Mol. Spectrosc.* **2001**, *206* (1), 33−40.
(39) Cooke, S. A.; Gerry, M. C. L. *Phys. Chem. Chem. Phys.* **2004**, *6* (13), 3248−3256.
(40) Mikhailov, V. A.; Tew, D. P.; Walker, N. R.; Legon, A. C. *Chem. Phys. Lett.* **2010**, *499* (1−3), 16−20.
(41) Walker, N. R.; Tew, D. P.; Harris, S. J.; Wheatley, D. E.; Legon, A. C. *J. Chem. Phys.* **2011**, *135* (1), 014307.
(42) Evans, C. J.; Reynard, L. M.; Gerry, M. C. L. *Inorg. Chem.* **2001**, *40* (24), 6123−6131.